

Cite this: *Nanoscale*, 2012, **4**, 5268

www.rsc.org/nanoscale

Growth and properties of coherent twinning superlattice nanowires

Erin L. Wood^a and Frederic Sansoz^{*ab}

Received 23rd May 2012, Accepted 10th July 2012

DOI: 10.1039/c2nr31277h

Although coherent twin boundaries require little energy to form in nanoscale single crystals, their influence on properties can be dramatic. In recent years, some important steps forward have been made in understanding and controlling twinning processes at the nanoscale, making possible the fabrication of nanoengineered twinning superlattices in crystalline nanowires. These advances have opened new possibilities for properties and functionalities at the atomic and quantum scales by modulating twin densities. This article presents a brief overview of recent theoretical and experimental progress in growth mechanisms and promising properties of coherent twinning superlattice nanowires with special emphasis toward cubic systems in semiconductor and metallic materials. In particular, we show how nanoscale growth twins can considerably enhance bandgap engineering and mechanical behaviour in quasi-one-dimensional materials. Opportunities for future research in this emerging area are also discussed.

Introduction

The fundamental study of size, surface structure, and interface effects on material properties in semiconductor and metallic nanowires (NWs) is of paramount importance for current

nanotechnology applications in electronics, optoelectronics, thermoelectrics, photonics, mechanical systems, and life sciences. Over the past decade, many research studies have been devoted to the growth of nanoscale twins in crystalline NWs, and their role on physical and mechanical properties at the molecular scale. In pure cubic systems and zinc-blende binary alloys in semiconductors and metals, a twin boundary is a zero-stress interface characterized by a single $\{111\}$ -oriented hexagonal-close-packed layer with no dangling bonds, as shown in Fig. 1. At the atomic scale, these unique characteristics confer the maximum degree of symmetry

^aMechanical Engineering Program, School of Engineering, The University of Vermont, Burlington, VT 05405, USA. E-mail: frederic.sansoz@uvm.edu; Tel: +1 802-656-3837

^bMaterials Science Program, The University of Vermont, Burlington, VT 05405, USA



Erin L. Wood

Erin Wood is a doctoral student in mechanical engineering with the School of Engineering at the University of Vermont in the United States. She earned a B.S in Chemistry in 2005 from Chatham College, and a M.S in Industrial Chemistry in 2009 from the University of Central Florida. Her current research focuses on the growth and mechanical properties of coherent twinning superlattices in metallic nanowires.



Frederic Sansoz

Frederic Sansoz is an associate professor in mechanical engineering and materials science with the School of Engineering at the University of Vermont in the United States. Dr Sansoz earned an engineer diploma in mechanical and aerospace engineering and M.S. in materials science and engineering from the Ecole Nationale Supérieure de Mécanique et Aérotechnique in Poitiers, France in 1996, and a Ph.D. with Honors in materials science and engineering from Ecole des Mines de Paris in 2000. His current interest focuses on examining how size, microstructure (in particular, twin boundaries) and surface structure can influence mechanical and thermoelectric properties in low-dimensional materials at the nanoscale.

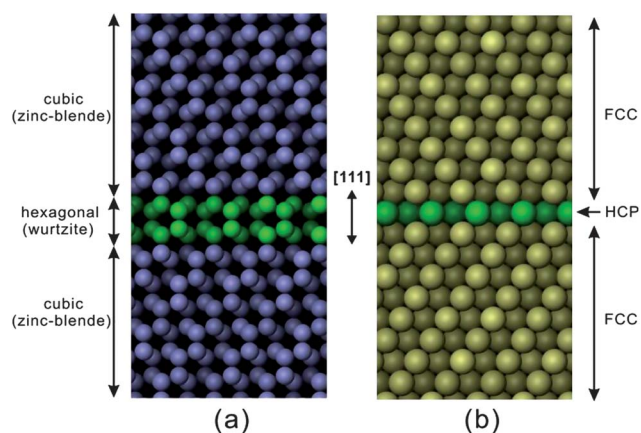


Fig. 1 Atomic structure of coherent twin boundaries (in green colour) in (a) diamond-cubic and zinc-blende semiconductors, and (b) face-centred cubic (FCC) metals. Twins are parallel to $\{111\}$ planes with either wurtzite or hexagonal-close-packed (HCP) arrangements.

and coherency to twin boundaries in comparison to other types of grain boundaries. In addition, twinning can occur easily during crystal growth at the nanoscale,¹ and requires very little energy to form. Interestingly, the occurrence of twinning defects has been a long-standing issue in limiting the yield of single crystals in bulk semiconductors obtained by traditional melt-recrystallization process.² By contrast, recent advances have enabled the fabrication of coherent twinning superlattices in a vast array of quasi-one-dimensional nanostructures by promoting and tuning the growth of twin boundaries at the nanoscale. Forming well-ordered, periodic distributions of twin boundaries, however, remains challenging and largely dependent upon the system being synthesized as shown below. Therefore, gaining predictive understanding on the processes of twin nucleation in NWs, and their underlying mechanisms, is critical for future investigations of properties and applications related to twinning superlattice NWs. This Feature Article presents an overview of recent progress in growth mechanisms and structure–property relationships in coherent twinning superlattices NWs with particular focus on relevant cubic systems in semiconductor and metallic materials. We note that mechanisms and properties in superlattice heterostructures made of two or more materials have already been discussed in an earlier review,³ and therefore are not addressed here.

Semiconductor nanowires

Growth mechanisms

Past experimental studies have shown supporting evidence that twinning is ubiquitous in nanoscale semiconductors. For example, twin boundaries have been observed in various types of semiconductor NWs, such as Group III–V NWs,^{4–19} Group II–VI NWs,^{20–22} pure Si NWs,^{23–25} carbide NWs,^{26–30} and oxide NWs.^{31–34} Notably, control over periodic twin ordering has been more systematically investigated in zinc-blende III–V NWs such as GaP, GaAs, InP, and InAs NWs.^{4–18}

The primary chemical method to synthesize nanoscale twins in semiconductor NWs is the vapour–liquid–solid (VLS) growth. A concrete example of perfect twinning superlattice in a

VLS-grown InAs NW¹⁶ is shown in Fig. 2a. This approach uses a metal seed particle in order to decompose a vapour-phase reactant into a semiconductor through a liquid eutectic alloy at high temperature as shown in Fig. 2b. The liquid alloy droplet subsequently crystallizes into a solid NW when the seed metal becomes saturated with the semiconductor. Similarly, the supercritical fluid–liquid–solid approach has been used to grow NWs in supercritical solvents, where twinning is also found to be prominent at high temperatures.¹⁰ Twin boundaries obtained from these methods are typically aligned perpendicularly to the NW axis along the $\{111\}$ direction, as illustrated in Fig. 2c. Such NWs exhibit two primary morphologies: cylindrical NWs with hexagonal cross section made of $\{121\}$ surface facets and random twin boundary spacing (TBS), or zigzag NWs with $\{111\}$ surface facets and more constant TBS. It should be noted, however, that $\{111\}$ microfaceting is predicted to disappear for very small diameters (*e.g.* <10 nm in GaP NWs).¹⁰

The ease of cubic systems to form twin boundaries can be understood by considering a layer-by-layer growth process on $\{111\}$ planes, and by the fact that the twin formation energy in these materials is about only half the stacking-fault energy and generally less than the thermal energy, $k_{\text{B}}T$ where k_{B} is the Boltzmann constant.^{10,27} For instance, for a typical growth temperature of 500 °C, $k_{\text{B}}T \sim 72$ meV, which is significantly larger than the twinning energy for most III–V semiconductors.¹⁰ Surface energies also provide another reason for twin nucleation in NWs. $\langle 111 \rangle$ -grown semiconductor crystals are usually bound by six $\{121\}$ surface facets; however, these facets can be seen at atomic level as a series of $\{111\}$ microfacets with correcting steps. Consequently, simultaneous growth of twin boundaries and zigzag $\{111\}$ microfacets promotes a lower state of energy in the NW because surface energies are higher for $\{121\}$ facets with steps than for $\{111\}$ microfacets with intervening twin boundaries.

Furthermore, TBS is observed to decrease significantly as the growth temperature and vapour pressure increases,^{8,11,18} or as the diameter decreases.^{20,35} Also, in Group III–V NWs, the precursor V/III ratio in the vapour phase is found to play an important role in the defect density.³⁶ In turn, these parameters can affect the chemical potential, $\Delta\mu$, and the energies at the liquid–solid interface, the solid–vapour interface, and the liquid–vapour interface, γ_{LS} , γ_{SV} and γ_{LV} , respectively (Fig. 2b). Johansson *et al.*⁸ first noted that certain elements from the vapour phase have low solubility in the metal seed. Therefore growth of semiconductor NWs has to proceed from the edge of the NW–seed interface, so called three-phase boundary (TPB), where all species can be made available for the growth. Using classical nucleation theory, these authors proposed to model the energy barrier for nucleation of a semi-circular twin nucleus of radius r and height h at the TPB, ΔG_{T} , as the sum of the nucleus energy of a $\{111\}$ plane, the twinning energy and the energy of the surface step associated with the nucleus. Therefore, it can be derived that

$$\Delta G_{\text{T}} = -\frac{\pi}{2}r^2\left(\frac{\Delta\mu}{S_{\text{c}}} - \gamma_{\text{T}}\right) + (\pi\gamma_{\text{LS}} + 2\gamma_{\text{SV}})rh \quad (1)$$

where S_{c} is the inverse of the nucleation site density on $\{111\}$ planes and γ_{T} is the twin energy (Fig. 2e). It was shown that, since γ_{T} is generally small compared to $\Delta\mu/S_{\text{c}}$, the energy barriers for twin nucleation and ordinary nucleation are not significantly

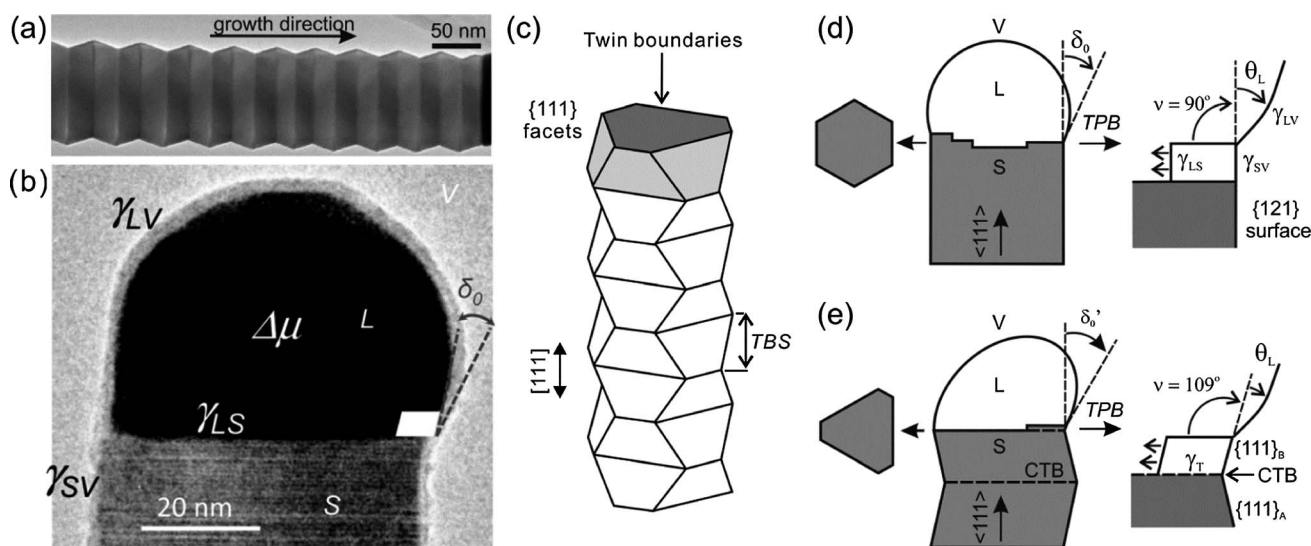


Fig. 2 Vapour-liquid-solid (VLS) model of lamellar twin growth in $\langle 111 \rangle$ -oriented semiconductor NWs. (a) VLS-grown InAs NW exhibiting well-controlled twinning and $\{111\}$ microfaceting from Dick *et al.*¹⁶ reprinted with permission from IOP Publishing. (b) Layer growth at the three-phase boundary (TPB) in GaP NWs from Algra *et al.*¹⁸ reprinted with permission from American Chemical Society. The catalyst particle can be seen in dark colour. δ_0 is the contact angle between liquid droplet and tip at the TPB. (c) Schematic of $\langle 111 \rangle$ -grown twinned NWs with zigzag $\{111\}$ microfacets and periodic twin boundary spacing (TBS). (d) Layer-by-layer growth mechanism in NWs with $\{121\}$ surface facets. (e) Mechanism of twin nucleation in NWs with zigzag $\{111\}$ microfacets. Illustration adapted from Davidson *et al.*¹⁰ with permission from American Chemical Society.

different.⁸ Therefore random twinning in semiconductor NWs can be interpreted from fluctuations in mass-transport to the TPB, as well as from thermal fluctuations,⁷ especially at high temperatures. However, neither periodic twin ordering nor decrease in TBS with increasing vapour partial pressure, which primarily relates to a change in γ_{LV} ,¹⁸ can be accounted for using eqn (1). Davidson *et al.*¹⁰ and Algra *et al.*^{11,18} proposed to refine this idea by considering the interfacial tension at the TPB and the deformation of the liquid particle during crystal growth. By way of illustration, Fig. 2d schematically depicts the growth process of a VLS NW without twin boundaries. As mentioned above, in the absence of twins, semiconductor NWs exhibit straight $\{121\}$ facets and keep a perfectly hexagonal shape during growth. Accordingly, it can be assumed for this type of NWs that all facets make a right angle with respect to the TPB ($\nu = 90^\circ$ in Fig. 2d) at all time. Furthermore, the contact angle between the liquid droplet and the tip, δ_0 , is at equilibrium whether twin boundaries are formed or not. Therefore, according to Davidson *et al.*,¹⁰ the wetting angle θ_L between the droplet and the NW sidewall is mostly constant during growth, and equal to

$$\theta_L = \arccos\left(\frac{\gamma_{SV}^2 + \gamma_{LV}^2 - \gamma_{SL}^2}{2\gamma_{SV}\gamma_{LV}}\right) \quad (2)$$

It is therefore clear from eqn (2) that the liquid-vapour interface energy is as important as the other interface energies for twin nucleation. The growth of twinned NWs takes place differently because the angle formed by $\{111\}$ microfacets with respect to the TPB is either acute ($\nu = 71^\circ$) or obtuse ($\nu = 109^\circ$), as represented in Fig. 2e. As such, the NW cross-sectional shape continuously evolves from hexagonal to triangular during growth, which dramatically increases the surface tension on the liquid. This effect causes the droplet to deform asymmetrically and the wetting angle to change, which governs the process of

twin nucleation. More specifically, both angles θ_L and δ_0 tend to increase if the facet angle is acute. This scenario may stop the NW growth because, if the angle becomes too large, the droplet can no longer dewet the surface at the TPB. On the contrary, if the facet angle is obtuse, the wetting angle θ_L decreases during growth. In this case, dewetting of the tip may occur, which could ultimately inhibit the growth process as well. Therefore, twin nucleation coupled to a change in facet orientation is necessary to reduce the surface tension caused by the change in morphology at the droplet-NW interface. Furthermore, by using literature values for the surface energies of different Au seeded semiconductor NW systems, Davidson *et al.*¹⁰ have shown that, while the equilibrium contact angle between droplet and NW does not significantly change between different semiconductors, θ_L varies notably. For example, twinning occurs easily in Au-seeded III-V NWs, as opposed to Au-seeded Si NWs with $\langle 111 \rangle$ growth direction, because θ_L is significantly smaller in the latter, which facilitates dewetting at the TPB without twin formation. Nevertheless, it was shown that twinning can be observed experimentally in Si NWs by substituting the seed metal with Cu instead of Au.²³ Also, a past theoretical study comparing twinning between different III-V semiconductor NWs³⁷ predicted that TBS decreases with increasing ionicity, which is consistent with the reduction in energy barrier for twinning with increasing $\Delta\mu$ in eqn (1). Furthermore, it was hypothesized that surface oxidation creates a protective shell that restrains lateral growth, which may help in keeping TBS more uniform along the NW length.²²

Bandgap engineering

Engineering of quantum properties is an important goal in semiconductor nanotechnology for next-generation electronic,

optoelectronic, and thermoelectric devices. Here we examine how twinning superlattices influence these properties in semiconductor NWs when TBS, twin distribution, and surface faceting vary. It is worth noting that, although twinning and microfaceting effects are mutually dependent in quasi-one-dimensional nanostructures, their roles on properties are distinct. Because electronic band structures can differ markedly between hexagonal and cubic crystals in semiconductors, twin interfaces have a direct impact on bandgap and band profiles due to their unique structure as hexagonal monolayers. For example, the bandgap energy is smaller in hexagonal Si (Si IV) than in cubic Si (Si I), and the minimum potential of the conduction band generally exhibits lower energy in Si IV than in Si I with a net difference of -0.109 eV.²³ Therefore, the potential difference between these two Si phases acts as if each twin boundary was a quantum well, as schematically illustrated in Fig. 3b.

In turn, this effect could make possible the confinement of electrons similar to the behaviour of quantum dots.³⁸ Although twinning defects have proved to diminish coherent electron transport,³⁹ modulating the distribution of quantum wells by twinning superlattices in NWs opens new possibilities for augmenting Seebeck effect with little to no sacrifice on electrical conductivity, which could dramatically boost thermoelectric performance and figure-of-merit in Si NWs for miniaturized cooling and energy conversion.^{23,40,41} In an opposite way, both bandgap and conduction band potentials in InP NWs increase from zinc-blende to wurtzite phases, which results in the creation of quantum barriers ($+0.129$ eV)¹² as shown in Fig. 3c. Experimentally, such quantum barriers were found to decrease carrier mobility in periodically twinned III–V NWs compared to defect-free NWs.^{14,17} However, photo-excited electrons in this type of twinned NWs can reach much higher energy levels due to the

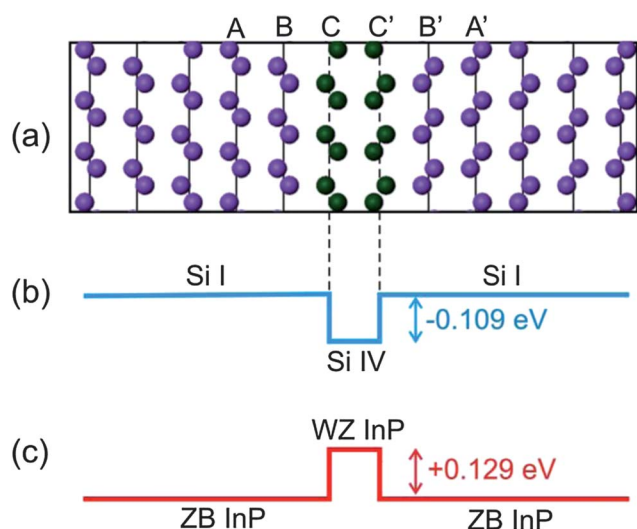


Fig. 3 Twin boundary effects on electronic band structure in semiconductors. (a) Atomic configuration of a twin showing the hexagonal and cubic structures in green and purple colours, respectively. Minimum of the conduction band potential across twin plane (b) in Si where the net difference in energy between hexagonal Si (Si IV) and cubic Si (Si I) is negative, thereby giving rise to a quantum well,²³ and (c) in InP where the wurtzite (WZ)–zinc-blende (ZB) energy difference is positive, and acts as a quantum barrier.¹²

multiple wurtzite domains, thus causing significant wavelength shift in photoluminescence and cathodoluminescence experiments.^{12,15,21,22} It was found, for example, that twinning superlattices produce blue and red shifts in the photoluminescence spectrum of InP NWs¹² and ZnTe NWs,²¹ respectively. This means that a direct correlation between twin density and optical properties can be obtained with coherent twinning superlattice NWs, which holds great promise for optoelectronics and solar cell applications.^{22,42} Strain engineering offers an additional possibility to control electronic properties in periodically twinned NWs. Past first-principles simulation studies have revealed that twin boundaries in NWs are somewhat transparent to electron transport.^{43–45} However, Tsuzuki *et al.*⁴³ have found that applying an external strain along the NW axis can significantly shift the bottom of the conduction band in the quantum barriers associated with twin boundaries, and that different electronic properties can rise by tuning both the applied strain and TBS in InP NWs. This phenomenon stems from inhomogeneous stress fields caused by twinning and surface faceting under an applied strain, which locally affects the conduction and valence band potentials.

Mechanical and thermal transport properties

It is well established that the mechanical behaviour of semiconductor NWs is quasi brittle. Therefore, for brittle ceramic materials such as SiC, the relevant parameters are only the Young's modulus and the yield strength. Based on past atomistic simulation studies, there is good agreement in the literature that twinning moderately increases the elastic modulus with decreasing TBS in SiC NWs,^{29,46} although elastic properties in other twinned NW systems remain largely unexplored. However, some conflicting observations exist in the relationship between twinning and strength because it was reported that addition of twins can both increase and decrease the ultimate strength of SiC NWs compared to twin-free SiC NWs.^{46–48} This discrepancy can be interpreted by the possible dispersion in mechanical strength due to differences in surface morphology.^{49,50} It was also predicted theoretically that nucleation of cracks on a zinc-blende NW is made easier due to the stress singularities that occur at the intersection of two opposing $\{111\}$ facets.⁴⁹

Similarly, Sansoz predicted in a recent atomistic simulation study that surface faceting associated with $\{111\}/\{100\}$ sawtooth facets significantly decreases thermal conductivity in Si NWs.⁵¹ This result suggests that periodic twinning may also play an indirect role in thermal transport characteristics due to surface effects. In particular, this idea is supported by recent experimental measurements in individual InAs NWs with random twin defects showing a two-order reduction in thermal conductivity compared to bulk.⁵² However, since any reduction in thermal conductivity is critical for improving the thermoelectric figure-of-merit of nanoscale semiconductors,^{40,41} further experimental and theoretical progress is required to fully assess the impact of twin boundaries on thermal transport behaviour in semiconductor NWs.

Metallic nanowires

Twinning in electrodeposited nanowires

Electrodeposition (ED) is a well-established technique for the fabrication of metallic NWs with submicron diameters.^{53–58} Size

reduction in ED NWs is obtained by directly electroplating metals inside a solid template containing nanoscale cylindrical pores. Standard templates are either anodized aluminium oxide films with dense, hexagonally arranged pores, or track-etched polycarbonate membranes with smaller porosities. Microstructure, morphology, and texture of ED NWs are generally controlled by the applied potential or current density, the bath composition, and the pore size and shape.

Twinning has been observed in ED NWs primarily made of Cu, Au and Ag. Evidence of twinning was reported from as early as 2001⁵⁹ in Cu NWs produced by direct-current ED. Twin boundaries were observed with a salt bath consisting only of $\text{CuSO}_4 \cdot \text{H}_2\text{O}$ and H_2SO_4 , which exhibited increased conductivity in comparison to the other electrolytes used. However, it was speculated that, due to observations of surface steps formed on the NWs, twins could result from plastic deformation and slip, instead of being growth twins. More recently, it was found that optimizing both the bath composition and the applied current density *via* pulsed ED was successful in synthesizing twinned ED Cu nanopillars with a diameter of 500 nm.⁶⁰ These nanopillars featured a [111] growth orientation and dense distributions of planar twins (TBS ~ 9 nm). Similarly occasional twinning has been observed in Ag NWs⁶¹ with certain electrolytes under alternating-current ED. Ag NWs with a [220] growth direction and lengthwise (111)[112] twins were also observed by Wang *et al.*⁶² However, the properties for this type of lengthwise twinning are not part of this review. In Au NWs, Tian *et al.*⁵⁸ used 1–2% gelatin as an additive to increase pore wetting, and observed [111]-oriented Au NWs with random lamellar twinning. After further investigation by Wang *et al.*⁶³ These NWs were found to present both primary (111)[112] and secondary ($\bar{1}\bar{1}$)[112] twin boundaries. Karim *et al.*⁶⁴ found (111) twins in single-crystalline [110] Au NWs grown under potentiostatic conditions.

To this date, however, higher twin densities have only been observed in metallic NWs synthesized by non-templated ED, or direct ED method. Remarkably, Zhong *et al.*⁶⁵ recently reported Cu NWs grown by direct ED on a glass substrate with TBS as small as 0.5 nm and an average diameter >100 nm (Fig. 4a). Although direct ED makes the control of diameter more elusive, the lack of post-synthesis processing steps such as template dissolution assures that these twins are all growth twins.

There is also some experimental evidence of growth twins in Ag NWs obtained by direct ED.^{66,70} Such Ag NWs were initially grown as dendrite structures as shown in Fig. 4b and c. Upon relaxation, however, the dendrite arms fell off through a possible electrochemical Ostwald ripening process. Bamboo-like twinned Ag NWs were also produced by the same approach under high DC potentials and uniform magnetic fields.⁷¹ While no branching was visible, the NWs exhibited twinning in the narrowest areas.

Twinning *via* other synthetic methods

Chemical reduction techniques are also increasingly popular for producing metallic NWs. A five-fold twinning about the axis of growth is a common twinning motif in FCC NWs, and has been observed in Au, Ag, Pd, Cu, and Fe.^{72–76} Evidence of twinning superlattices obtained by wet chemical methods or physical vapour deposition is more limited, but the number is growing in the literature. Several representative examples are shown in

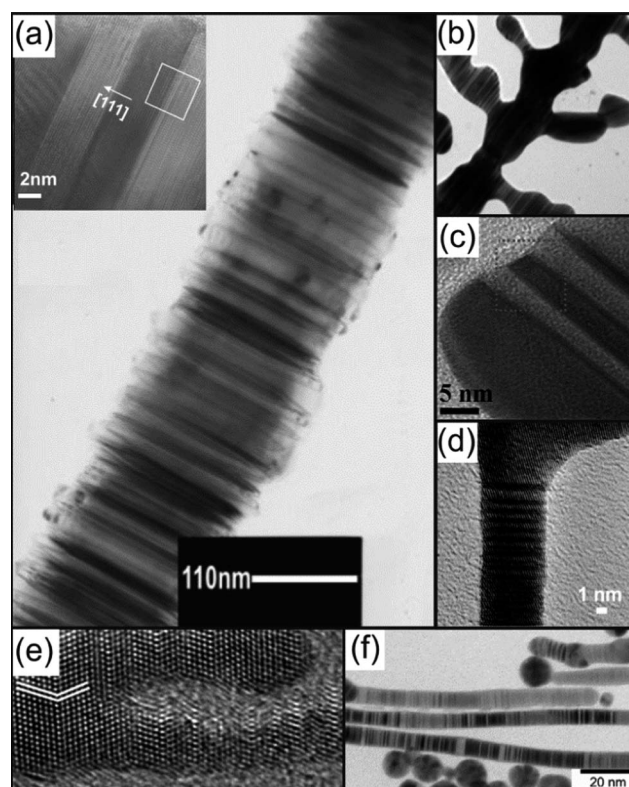


Fig. 4 Coherent twinning superlattices in FCC metal NWs formed by different methods. (a) Cu NW obtained by binary interface stress during non-templated electrodeposition, a magnified view of twin boundaries is shown in inset (reprinted with permission from ref. 65 ©Wiley-VCH 2009). (b) Ag nanostructure obtained through ion migrational-transport-controlled 3D electrodeposition with (c) magnified view of twinning (reproduced from ref. 66). Au NWs obtained through (d) mechanical disturbance (reprinted with permission from ref. 67 ©American Chemical Society 2010), (e) oriented-attachment of nanoparticles (reprinted with permission from ref. 68 ©Wiley-VCH 2007), and (f) surface ligand rearrangement (reprinted with permission from ref. 69).

Fig. 4d–f. Au NW networks grown in microemulsions have been shown to have lamellar twinning characteristics.⁷⁷ Also, ultrathin (<10 nm) Au NWs synthesized through a variation of the oleylamine reduction technique exhibited lamellar twinning. Halder and Ravinshankar⁶⁸ first reported twinning in ultrathin Au NWs (Fig. 4e). Later, Bernardi *et al.*⁶⁹ reported a method modification producing straight NWs with no branching and extensive twin boundaries (Fig. 4f). Twinning was also observed in similarly synthesized NWs, but under mechanical disturbance through stirring that promoted a bent structure.^{67,78} Twin boundaries were exclusively seen near the elbows (Fig. 4d), which therefore makes it unclear whether they were growth twins or deformation twins. Other types of twinned structures in Ag such as Ag rice-shaped nanoparticles with a high density of lattice defects were synthesized through a polyol process.⁷⁹ These structures were predominately FCC with some HCP phase near the tips. The FCC phase exhibited dense lamellar twins along the [111] direction. A similar structure was found in Ag heterostructures formed in the presence of a surfactant and a mild reducing agent.⁸⁰ The reaction produced a wire like needle section conjoined with a much thicker rod-like section. These

heterostructures also contained both FCC and HCP phases with high densities of lattice defects in the needle section. Furthermore, it is common to find Cu NWs produced by physical vapour deposition forming twin boundaries, as well as flat {100} and {111} facets, during growth.^{81,82}

Proposed growth mechanisms

Although there exists no general consensus to comprehensively explain the process governing twin nucleation in metallic NWs, two possible mechanisms have been envisioned so far. On one side, Halder and Ravishankar⁶⁸ proposed the oriented attachment of nanoparticles for the growth of twinned Au NWs by oleylamine reduction. These authors suggested that Au cations are first reduced with an amine to form Au nanoparticles with {111} and {100} facets. These faceted nanoparticles are capped with the amine group; however preferential binding to the {100} facets takes place. When ascorbic acid is added to the growth solution, the {111} facets are deprotected and {111} facets from two particles can bind together and fuse in a chain-like manner to build NWs. The formation of twin boundaries during the fusion of {111} facets is energetically possible, and consistent with the creation of {111}/{100} sawtooth facets. This hypothesis is also supported by the existence of branched NWs and NWs with zigzag morphology. Oriented attachment of nanoparticles is also alluded for the twinning structures seen in Ag nano-rice.⁷⁹ Sun *et al.*⁷¹ also suggested that, based on observations of the irregular cross-sectional shape and polyhedral surface morphology, twinned Ag NWs grown through direct ED process under a magnetic field could result from the aligned attachment of smaller Ag nanoparticles.

On the other side, Bernardi *et al.*⁶⁹ proposed a layer-by-layer growth model with ligand rearrangement at the free surface. This mechanism is shown to be favoured when twin boundary formation is less than the energy for ligand rearrangement, which could occur in systems with low stacking-fault energy such as Au, when coupled with large, bulky asymmetric ligands such as oleylamine. In ED NWs, Wang *et al.*⁶³ also alluded that during deposition with a correct stacking sequence of ABCABCABC, adatoms will preferentially seek to deposit on the next correct plane. For example, if an A plane was last formed, adatoms will seek a B site; however additives do not have this preference and may force the adatom to bind instead to a C site. The energy difference between the B and C sites is small, so this process is not detrimental energetically. Furthermore, Zhong *et al.*⁶⁵ suggested in their direct ED experiments that perhaps twinning is dependent on an ionic flux at the liquid–solid interface. Formation of twins or stacking faults could then be due to fluctuations in ion-transport at this interface.

Mechanical properties

Metallic NWs are central building blocks in photonic and electronic nanodevice fabrication because of their unique electrical and optical properties at the nanoscale. Yet it is imperative for device reliability to employ materials with excellent mechanical properties without sacrificing their desired function, which is made possible with nanotwinned materials. For example, past studies on bulk metals have proved that nanoscale twins can

significantly increase mechanical strength and plasticity without disrupting electrical conductivity in the same way that other types of grain boundaries do.^{83,84} Also, past reports in the literature tend to indicate that twinning does not change the plasmonic response of NWs, which agrees with the trend that the plasmonic resonance bands of metals such as Au and Ag is predominantly size-related.^{85,86} Also, early experimental studies showed that twin planes do not significantly affect the Young's modulus of metallic NWs and nanorods.⁸⁷ Nevertheless, examining the role of nanoscale twins on mechanical strength and plastic deformation in metallic NWs has become a focal point of research over the last few years,⁸² primarily because past experimental and theoretical studies in FCC metal NWs have shown clear evidence that, among all types of microstructures (*e.g.* nanocrystalline, polycrystalline with twins, *etc.*), twinning superlattice NWs are the strongest.^{60,88,89} For example, pronounced increases in strength were measured in direct ED Cu NWs and ED Cu nanopillars with lamellar twinning.^{60,65} Even with large diameters (>200 nm), ED Cu NWs and nanopillars exhibited a three-fold increase in ultimate tensile strength compared to bulk Cu materials, with no significant change in electrical properties.⁶⁵ Bernardi *et al.*⁶⁹ also measured the yield strength of ultrathin Au NWs with twins by using ultrasonication, and estimated their tensile strength to be ~ 1.63 GPa, much higher than that of single-crystalline Au NWs with an equivalent diameter (600 MPa). However experimental strength measurements in twinned NWs are scarce because it is, in general, extremely challenging experimentally to characterize the mechanical properties of NWs with small diameters.⁹⁰

Surprisingly, past atomistic simulation studies on the plasticity of metallic NWs under uniform deformation revealed that twin boundaries do not always strengthen NWs compared to twin-free NWs.^{82,91–95} Our previous computer simulations using classical molecular dynamics have shown, in particular, that several factors such as TBS,^{88,93,94,96} the ratio of diameter over TBS,⁹⁷ the stacking-fault energy of the metal,⁹⁸ and the surface morphology such as surface facets^{88,99} must be carefully designed to produce strengthening in periodically twinned metallic NWs. In particular, pronounced strain-hardening effects and plastic deformation due to the blockage of dislocations by twin boundaries was seen in Au NWs as TBS decreases, which differs markedly from the brittle failure in twin-free Au NWs of same diameter (Fig. 5a).⁹⁷

Computer simulations also showed that the failure mode in circular Au NWs changes fundamentally from brittle-like to extended plasticity with strain hardening when a critical ratio of diameter over TBS is exceeded. Such noticeable increase in ductility could serve an important role as a fail-safe approach to prevent catastrophic failure of NWs under applied stresses. This phenomenon occurs because partial dislocations, which are usually emitted from the free surface in the absence of internal defects,^{100,101} are blocked by pre-existing twin boundaries, as shown in Fig. 4b. The blocked dislocations can only transmit through the twin when the stress is strong enough to activate trailing partial dislocations.^{97,98} Therefore, the stress required to emit surface dislocations must be lower than the stress necessary to transmit partial dislocations through twin interfaces in order to observe strain hardening. Interestingly, if the applied stress decreases before blocked dislocations can transmit through

coherent twin boundaries, dislocations could be reabsorbed by the surface, and leave a pristine NW upon unloading, somewhat reminiscent to a self-healing process.⁹⁷ Also, strengthening effects in twinned Au NWs can be very strong, because their unstable stacking energy and stress for dislocation nucleation are low. On the contrary, in metals with high unstable stacking energies such as Cu and Ni, twinned NWs remain brittle. Another salient feature is that the surface morphology like $\{111\}$ zigzag facets, can dramatically improve the strength of twinned Au NWs as shown by the results of Deng and Sansoz⁸⁸ presented in Fig. 2c. It was shown that the stress to nucleate new surface dislocations rises more dramatically as TBS decreases with zigzag $\{111\}$ facets, because of the nucleation of Lomer (001)[110] dislocations, instead of partial dislocations commonly observed in FCC metals.^{88,99} Ultimately, this synergistic influence of twin, size and surface faceting on plastic deformation mechanisms enables zigzag metallic NWs to approach the theoretical limit of strength, which is more than 45 times larger than the bulk strength for Au, as shown for twinned Au NWs in Fig. 5c.

Summary and outlook for future research

This brief overview has clearly shown that coherent twinning superlattices hold great promise for tuning and enhancing physical and mechanical properties in crystalline NWs without compromising one property over another. Although semiconductor and metallic NWs exhibit different properties aiming at diverse applications, the conclusions of this survey point to some commonalities between the two systems. For instance, it is evident that a strong relationship exists between twinning and surface effects in growth of NWs. In VLS-grown semiconductor NWs, controlling the deformation of the liquid droplet was found critical in achieving perfectly periodic twin ordering. Because $\{111\}$ microfaceting is associated with twin nucleation, microfacets greatly contribute to the droplet deformation. Like semiconductor NWs, $\{111\}$ microfaceting has also been observed in metallic NWs with high twin densities.⁶⁸ While twinning has been observed in metallic NWs from templated ED, non-templated ED and chemical reduction techniques have yielded better results in terms of achieving high twin densities, perhaps owing to the lack of rigid constraint on the growing surfaces. In non-templated ED NWs, in particular, it is crucial to further understand the fundamental role of fluctuations in transport at the liquid–solid interface in order to fully control their microstructure. Furthermore, achieving regular TBS is important because properties are found to change significantly as a function of twin density in both systems. For example, stress for surface dislocation nucleation, which is important for strengthening effects in twinned NWs, varies linearly with the number of twin boundaries per unit length, $1/\text{TBS}$;^{93,96} and NWs will fail on the segment with largest TBS.⁹³ Therefore, uniform twin distributions give rise to better tensile strength. Similarly, modulating twin density in semiconductor NWs plays an important role in engineering bandgap and electronic behaviour at the quantum scale. Our ability to control twin densities is paramount for physical properties and functions such as optoelectronic and thermoelectric properties in twinned semiconductor NWs.

However, some progress still needs to be made in some areas. Future research in this emerging field can be summarized by asking the following questions. First, can perfect twinning superlattices be formed and controlled in metallic NWs? Unlike semiconductor NWs, a regular TBS has not been observed so far experimentally in metal NWs. A recent atomistic simulation study¹⁰² suggested a top-down approach using high-energy electron flux combined with torsion loading to guide the growth of twin boundaries in NWs; yet more simple synthetic methods are required. Likewise, twinning superlattices have not been synthesized in certain types of semiconductor NWs, such as Si NWs, which are also relevant for applications. Second, how to bridge the gap between experiments and theory to improve our fundamental understanding of growth and properties in coherent twinning superlattice NWs? In particular, computer simulations may help better understand the factor(s) governing twin nucleation and properties, however most computational studies have routinely focused on periodically twinned NWs, and rarely on more random twinning systems. Third, how does strain clearly affect properties in twinned NWs? For example, strain engineering could be exploited for designing electronic band

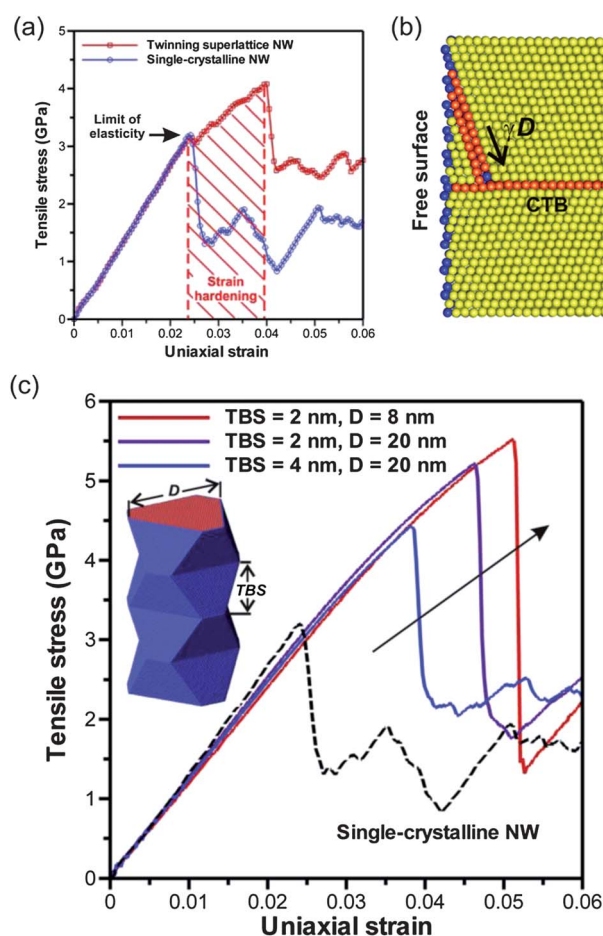


Fig. 5 Mechanical behavior of twinning superlattice NWs in Au predicted by molecular dynamics computer simulations. (a) Tensile stress–strain curves in twinned and twin-free Au NWs with a diameter of 12 nm. (b) Strain-hardening effects obtained by the blockage of partial dislocations emitted from the free surface by coherent twin boundaries (CTB). (c) Giant size-dependent strengthening due to synergistic effects between CTB and zigzag $\{111\}$ surface facets in Au NWs. The ultimate strength achieved in twinned zigzag Au NWs approaches the ideal strength of Au.

structures at twin interfaces in semiconductor NWs, which could be of particular interest for thermoelectric applications, although the effect of twinning in thermal transport behaviour remains largely unexplored, which also warrants further investigations.

Acknowledgements

This work was conducted under the auspices of grant DMR-0747658 from the National Science Foundation CAREER program.

Notes and references

- 1 A. S. Barnard, *J. Phys. Chem. B*, 2006, **110**, 24498–24504.
- 2 D. T. J. Hurle, *J. Cryst. Growth*, 1995, **147**, 239–250.
- 3 X. Fang, Y. Bando, U. K. Gautam, T. Zhai, S. Gradecak and D. Golberg, *J. Mater. Chem.*, 2009, **19**, 5683–5689.
- 4 F. M. Davidson, R. Wiacek and B. A. Korgel, *Chem. Mater.*, 2005, **17**, 230–233.
- 5 R. Banerjee, A. Bhattacharya, A. Genc and B. M. Arora, *Philos. Mag. Lett.*, 2006, **86**, 807–816.
- 6 L. D. Hicks and M. S. Dresselhaus, *Phys. Rev. B: Condens. Matter Mater. Phys.*, 1993, **47**, 12727–12731.
- 7 Q. Xiong, J. Wang and P. C. Eklund, *Nano Lett.*, 2006, **6**, 2736–2742.
- 8 J. Johansson, L. S. Karlsson, C. P. T. Svensson, T. Mårtensson, B. A. Wacaser, K. Deppert, L. Samuelson and W. Seifert, *Nat. Mater.*, 2006, **5**, 574–580.
- 9 G. Shen, Y. Bando, B. Liu, C. Tang and D. Golberg, *J. Phys. Chem. B*, 2006, **110**, 20129–20132.
- 10 F. M. Davidson, D. C. Lee, D. D. Fanfair and B. A. Korgel, *J. Phys. Chem. C*, 2007, **111**, 2929–2935.
- 11 R. E. Algra, M. A. Verheijen, M. T. Börgstrom, L. F. Feiner, G. Immink, W. J. P. van Enkevort, E. Vlieg and E. P. A. M. Bakkers, *Nature*, 2008, **456**, 369–372.
- 12 J. Bao, D. C. Bell, F. Capasso, J. B. Wagner, T. Mårtensson, J. Trägårdh and L. Samuelson, *Nano Lett.*, 2008, **8**, 836–841.
- 13 P. Caroff, K. A. Dick, J. Johansson, M. E. Messing, K. Deppert and L. Samuelson, *Nat. Nanotechnol.*, 2009, **4**, 50–55.
- 14 M. D. Schroer and J. R. Petta, *Nano Lett.*, 2010, **10**, 1618–1622.
- 15 Y. Ohno, *J. Electron Microsc. Tech.*, 2010, **59**, S141–S147.
- 16 K. A. Dick, P. Caroff, J. Bolinsson, M. E. Messing, J. Johansson, K. Deppert, L. R. Wallenberg and L. Samuelson, *Semicond. Sci. Technol.*, 2010, **25**, 024009.
- 17 C. S. Jung, H. S. Kim, G. B. Jung, K. J. Gong, Y. J. Cho, S. Y. Jang, C. H. Kim, C. W. Lee and J. Park, *J. Phys. Chem. C*, 2011, **115**, 7843–7850.
- 18 R. E. Algra, M. A. Verheijen, L. F. Feiner, G. G. W. Immink, W. J. P. van Enkevort, E. Vlieg and E. P. A. M. Bakkers, *Nano Lett.*, 2011, **11**, 1259–1264.
- 19 B. J. Ohlsson, M. T. Björk, M. H. Magnusson, K. Deppert, L. Samuelson and L. R. Wallenberg, *Appl. Phys. Lett.*, 2001, **79**, 3335–3337.
- 20 Q. Li, X. Gong, C. Wang, J. Wang, K. Ip and S. Hark, *Adv. Mater.*, 2004, **16**, 1436–1440.
- 21 Q. Meng, C. Jiang and S. X. Mao, *J. Cryst. Growth*, 2008, **310**, 4481–4486.
- 22 X. Fan, X. M. Meng, X. H. Zhang, M. L. Zhang, J. S. Jie, W. J. Zhang, C. S. Lee and S. T. Lee, *J. Phys. Chem. C*, 2008, **113**, 834–838.
- 23 J. Arbiol, A. F. I. Morral, S. Estrade, F. Peiro, B. Kalache, P. R. I. Cabarrocas and J. R. Morante, *J. Appl. Phys.*, 2008, **104**, 064312.
- 24 Z. W. Wang and Z. Y. Li, *Nano Lett.*, 2009, **9**, 1467–1471.
- 25 A. H. Carim, K. K. Lew and J. M. Redwing, *Adv. Mater.*, 2001, **13**, 1489–1491.
- 26 R. Wu, Y. Pan, G. Yang, M. Gao, L. Wu, J. Chen, R. Zhai and J. Lin, *J. Phys. Chem. C*, 2007, **111**, 6233–6237.
- 27 H. W. Shim, Y. F. Zhang and H. C. Huang, *J. Appl. Phys.*, 2008, **104**, 063511.
- 28 D. H. Wang, D. Q. Wang, Y. J. Hao, G. Q. Jin, X. Y. Guo and K. N. Tu, *Nanotechnology*, 2008, **19**, 215602.
- 29 V. G. Lutsenko, *Acta Mater.*, 2008, **56**, 2450–2455.
- 30 Z. J. Lin, L. Wang, J. Zhang, X. Y. Guo, W. Yang, H. K. Mao and Y. Zhao, *Scr. Mater.*, 2010, **63**, 981–984.
- 31 H. Chen, J. Wang, H. Yu, H. Yang, S. Xie and J. Li, *J. Phys. Chem. B*, 2005, **109**, 2573–2577.
- 32 X. Tao and X. Li, *Nano Lett.*, 2008, **8**, 505–510.
- 33 Y. Yang, R. Scholz, H. J. Fan, D. Hesse, U. Gösele and M. Zacharias, *ACS Nano*, 2009, **3**, 555–562.
- 34 C. C. Chang, J. L. Wu, N. H. Yang, S. J. Lin and S. Y. Chang, *CrystEngComm*, 2012, **14**, 1117–1121.
- 35 K. Sano, T. Akiyama, K. Nakamura and T. Ito, *J. Cryst. Growth*, 2007, **301–302**, 862–865.
- 36 H. J. Joyce, J. Wong-Leung, Q. Gao, H. H. Tan and C. Jagadish, *Nano Lett.*, 2010, **10**, 908–915.
- 37 T. Yamashita, K. Sano, T. Akiyama, K. Nakamura and T. Ito, *Appl. Surf. Sci.*, 2008, **254**, 7668–7671.
- 38 M. F. Crommie, C. P. Lutz and D. M. Eigler, *Science*, 1993, **262**, 218–220.
- 39 Z. G. Wang, S. J. Wang, C. L. Zhang and J. B. Li, *J. Nanopart. Res.*, 2011, **13**, 185–191.
- 40 A. I. Boukai, Y. Bunimovich, J. Tahir-Kheli, J. K. Yu, W. A. Goddard and J. R. Heath, *Nature*, 2008, **451**, 168–171.
- 41 A. I. Hochbaum, R. K. Chen, R. D. Delgado, W. J. Liang, E. C. Garnett, M. Najarian, A. Majumdar and P. D. Yang, *Nature*, 2008, **451**, 163–U165.
- 42 Y. Myung, J. H. Kang, J. W. Choi, D. M. Jang and J. Park, *J. Mater. Chem.*, 2012, **22**, 2157–2165.
- 43 H. Tszuzuki, D. F. Cesar, M. Rebello de Sousa Dias, L. K. Castelano, V. Lopez-Richard, J. P. Rino and G. E. Marques, *ACS Nano*, 2011, **5**, 5519–5522.
- 44 D. F. Li, B. L. Li, H. Y. Xiao and H. N. Dong, *Chin. Phys. B*, 2011, **20**, 067101.
- 45 D. Li, Z. Wang and F. Gao, *Nanotechnology*, 2010, **21**, 505709.
- 46 Z. G. Wang, J. B. Li, F. Gao and W. J. Weber, *Acta Mater.*, 2010, **58**, 1963–1971.
- 47 Z. Wang, X. Zu, F. Gao and W. J. Weber, *Phys. Rev. B: Condens. Matter Mater. Phys.*, 2008, **77**, 224113.
- 48 Z. Li, S. Wang, Z. Wang, X. Zu, F. Gao and W. J. Weber, *J. Appl. Phys.*, 2010, **108**, 013504.
- 49 R. Grantab and V. B. Shenoy, *Philos. Mag. Lett.*, 2011, **91**, 280–286.
- 50 J. Wang, C. Lu, Q. Wang, P. Xiao, F. Ke, Y. Bai, Y. Shen, X. Liao and H. Gao, *Nanotechnology*, 2012, **23**, 025703.
- 51 F. Sansoz, *Nano Lett.*, 2011, **11**, 5378–5382.
- 52 S. Dhara, H. S. Solanki, R. A. Pawan, V. Singh, S. Sengupta, B. A. Chalke, A. Dhar, M. Gokhale, A. Bhattacharya and M. M. Deshmukh, *Phys. Rev. B: Condens. Matter Mater. Phys.*, 2011, **84**, 121307.
- 53 C. R. Martin, *Science*, 1994, **266**, 1961–1966.
- 54 F. Maurer, J. Brötz, S. Karim, M. E. Toimil-Molares, C. Trautmann and H. Fuess, *Nanotechnology*, 2007, **18**, 135709.
- 55 M. Tan and X. Chen, *J. Electrochem. Soc.*, 2012, **159**, K15–K20.
- 56 M. Motoyama, Y. Fukunaka, T. Sakka and Y. H. Ogata, *Electrochim. Acta*, 2007, **53**, 205–212.
- 57 H. Pan, H. Sun, C. Poh, Y. Feng and J. Lin, *Nanotechnology*, 2005, **16**, 1559.
- 58 M. Tian, J. Wang, J. Kurtz, T. E. Mallouk and M. H. W. Chan, *Nano Lett.*, 2003, **3**, 919–923.
- 59 M. E. Toimil Molares, V. Buschmann, D. Dobrev, R. Neumann, R. Scholz, I. U. Schuchert and J. Vetter, *Adv. Mater.*, 2001, **13**, 62–65.
- 60 D. Jang, C. Cai and J. R. Greer, *Nano Lett.*, 2011, **11**, 1743–1746.
- 61 G. Sauer, G. Brehm, S. Schneider, K. Nielsch, R. B. Wehrspohn, J. Choi, H. Hofmeister and U. Gosele, *J. Appl. Phys.*, 2002, **91**, 3243–3247.
- 62 B. Wang, G. T. Fei, Y. Zhou, B. Wu, X. Zhu and L. Zhang, *Cryst. Growth Des.*, 2008, **8**, 3073–3076.
- 63 J. Wang, M. Tian, T. E. Mallouk and M. H. W. Chan, *J. Phys. Chem. B*, 2003, **108**, 841–845.
- 64 S. Karim, M. E. Toimil-Molares, F. Maurer, G. Mieke, W. Ensinger, J. Liu, T. W. Cornelius and R. Neumann, *Appl. Phys. A: Mater. Sci. Process.*, 2006, **84**, 403–407.
- 65 S. Zhong, T. Koch, M. Wang, T. Scherer, S. Walheim, H. Hahn and T. Schimmel, *Small*, 2009, **5**, 2265–2270.
- 66 C. Ding, C. Tian, R. Krupke and J. Fang, *CrystEngComm*, 2012, **14**, 875–879.

- 67 C. Wang, Y. Wei, H. Jiang and S. Sun, *Nano Lett.*, 2010, **10**, 2121–2125.
- 68 A. Halder and N. Ravishankar, *Adv. Mater.*, 2007, **19**, 1854–1858.
- 69 M. Bernardi, S. N. Raja and S. K. Lim, *Nanotechnology*, 2010, **21**, 285607.
- 70 J. Fang, H. Hahn, R. Krupke, F. Schramm, T. Scherer, B. Ding and X. Song, *Chem. Commun.*, 2009, 1130–1132.
- 71 S. Sun, D. Deng, C. Kong, Y. Zhang, X. Song, B. Ding and Z. Yang, *CrystEngComm*, 2011, **13**, 4827–4830.
- 72 H. Y. Wu, H. C. Chu, T. J. Kuo, C. L. Kuo and M. H. Huang, *Chem. Mater.*, 2005, **17**, 6447–6451.
- 73 Y. Sun, B. Mayers, T. Herricks and Y. Xia, *Nano Lett.*, 2003, **3**, 955–960.
- 74 X. Huang and N. Zheng, *J. Am. Chem. Soc.*, 2009, **131**, 4602–4603.
- 75 Y. Zhao, Y. Zhang, Y. Li and Z. Yan, *New J. Chem.*, 2012, **36**, 130–138.
- 76 T. Ling, H. Yu, X. Liu, Z. Shen and J. Zhu, *Cryst. Growth Des.*, 2008, **8**, 4340–4342.
- 77 M. Shen, Y. Du, P. Yang and L. Jiang, *J. Phys. Chem. Solids*, 2005, **66**, 1628–1634.
- 78 X. Hong, D. Wang and Y. Li, *Chem. Commun.*, 2011, **47**, 9909–9911.
- 79 H. Liang, H. Yang, W. Wang, J. Li and H. Xu, *J. Am. Chem. Soc.*, 2009, **131**, 6068–6069.
- 80 X. S. Shen, G. Z. Wang, X. Hong, X. Xie, W. Zhu and D. P. Li, *J. Am. Chem. Soc.*, 2009, **131**, 10812–10813.
- 81 J. Wang, H. Huang, S. V. Kesapragada and D. Gall, *Nano Lett.*, 2005, **5**, 2505–2508.
- 82 F. Sansoz, H. Huang and D. H. Warner, *JOM*, 2008, **9**, 79–84.
- 83 L. Lu, Y. Shen, X. Chen, L. Qian and K. Lu, *Science*, 2004, **304**, 422–426.
- 84 L. Lu, X. Chen, X. Huang and K. Lu, *Science*, 2009, **323**, 607–610.
- 85 J. Pérez-Juste, I. Pastoriza-Santos, L. M. Liz-Marzán and P. Mulvaney, *Coord. Chem. Rev.*, 2005, **249**, 1870–1901.
- 86 X. M. Sun and Y. D. Li, *Adv. Mater.*, 2005, **17**, 2626–2630.
- 87 H. Petrova, J. Perez-Juste, Z. Zhang, J. Zhang, T. Kosel and G. V. Hartland, *J. Mater. Chem.*, 2006, **16**, 3957–3963.
- 88 C. Deng and F. Sansoz, *ACS Nano*, 2009, **3**, 3001–3008.
- 89 F. Sansoz and V. Dupont, *Scr. Mater.*, 2010, **63**, 1136–1139.
- 90 Y. Lu and J. Lou, *JOM*, 2011, **63**, 35–42.
- 91 Y. Zhang and H. Huang, *Nanoscale Res. Lett.*, 2008, **4**, 34–38.
- 92 B. Hyde, H. Espinosa and D. Farkas, *JOM*, 2005, **57**, 62–66.
- 93 C. Deng and F. Sansoz, *Appl. Phys. Lett.*, 2009, **95**, 091914–091913.
- 94 K. A. Afanasyev and F. Sansoz, *Nano Lett.*, 2007, **7**, 2056–2062.
- 95 A. J. Cao, Y. G. Wei and S. X. Mao, *Appl. Phys. Lett.*, 2007, **90**, 151909.
- 96 C. Deng and F. Sansoz, *Scr. Mater.*, 2010, **63**, 50–53.
- 97 C. Deng and F. Sansoz, *Nano Lett.*, 2009, **9**, 1517–1522.
- 98 C. Deng and F. Sansoz, *Acta Mater.*, 2009, **57**, 6090–6101.
- 99 C. Deng and F. Sansoz, *Phys. Rev. B: Condens. Matter Mater. Phys.*, 2010, **81**, 155430.
- 100 H. Zheng, A. Cao, C. R. Weinberger, J. Y. Huang, K. Du, J. Wang, Y. Ma, Y. Xia and S. X. Mao, *Nat. Commun.*, 2010, **1**, 144.
- 101 Y. Lu, J. Song, J. Huang and J. Lou, *Nano Res.*, 2011, **4**, 1261–1267.
- 102 Y. Zhang and H. Huang, *J. Appl. Phys.*, 2010, **108**, 103507.